



**HAL**  
open science

## Rod like micellar structures in perfluorinated ionomer solutions

P. Aldebert, B. Dreyfus, G. Gebel, N. Nakamura, M. Pineri, F. Volino

► **To cite this version:**

P. Aldebert, B. Dreyfus, G. Gebel, N. Nakamura, M. Pineri, et al.. Rod like micellar structures in perfluorinated ionomer solutions. *Journal de Physique*, 1988, 49 (12), pp.2101-2109. 10.1051/jphys:0198800490120210100 . jpa-00210892

**HAL Id: jpa-00210892**

**<https://hal.science/jpa-00210892>**

Submitted on 4 Feb 2008

**HAL** is a multi-disciplinary open access archive for the deposit and dissemination of scientific research documents, whether they are published or not. The documents may come from teaching and research institutions in France or abroad, or from public or private research centers.

L'archive ouverte pluridisciplinaire **HAL**, est destinée au dépôt et à la diffusion de documents scientifiques de niveau recherche, publiés ou non, émanant des établissements d'enseignement et de recherche français ou étrangers, des laboratoires publics ou privés.

Classification  
Physics Abstracts  
61.12

## Rod like micellar structures in perfluorinated ionomer solutions

P. Aldebert (\*), B. Dreyfus, G. Gebel, N. Nakamura (\*\*), M. Pineri and F. Volino (\*)

Groupe Physico-Chimie Moléculaire, Service de Physique, Département de Recherche Fondamentale, Centre d'Etudes Nucléaires de Grenoble, 85X, 38041 Grenoble Cedex, France

(Reçu le 2 juin 1988, accepté le 18 août 1988)

**Résumé.** — Une structure en bâtonnets arrangés sur un réseau hexagonal est proposée dans des solutions et gels d'ionomères perfluorés. Deux différentes approches ont permis l'obtention du diamètre des bâtonnets. Le déplacement du pic d'interférence obtenu en diffusion aux petits angles permet de définir ce diamètre à partir de considérations géométriques. L'analyse du facteur de structure, sur des solutions très diluées, permet l'obtention directe du diamètre. Une bonne cohérence a été obtenue à partir de ces deux techniques d'analyse. Les rayons varient entre 18 et 31 Å selon la nature du solvant. Ces bâtonnets seraient formés par un noyau perfluoré plus ou moins organisé et les charges seraient rassemblées sur la surface. Le rayon ne dépend pas de la valeur de la constante diélectrique mais plutôt de la tension interfaciale entre le solvant et le polymère perfluoré. Ces structures pourraient correspondre à un état d'équilibre entre l'énergie élastique de déformation du groupe latéral et l'énergie interfaciale.

**Abstract.** — A hexagonal packing of rod like structures is proposed in solutions and gels of a perfluorinated ionomer. The diameter of the rods has been obtained by two different approaches either geometrical from shifts of the interference peak *versus* concentrations in small angle scattering experiments or direct from analysis of the structure factor in diluted solutions. Consistent results give values between 18 and 31 Å for the radius of the rods, depending on the solvent. The rods have a perfluorinated core with the charges on the surface and the diameter depends on the surface tension rather than on the dielectric constant of the solvent. The structure may result from a balance between elastic and interfacial energies as it is shown by calculations.

### 1. Introduction.

The aim of this paper is to bring new evidences concerning the rod like structure in solutions of perfluorinated ionomer membranes. A model of the structure involving the presence of such colloids had been proposed in a previous paper [1] from geometrical considerations associated with the ionomer peak shift *versus* concentration in small angle neutron and X-ray scattering experiments. The influence of the solvent, characterized by its dielectric constant and its surface tension, on the size of the rods will be studied here in order to define what is the driving force for the rod diameter. The form factor of the scattering objects will also be analysed at very high dilutions in order to have direct information on the

geometry and the diameter of the perfluorinated ionomer rods.

### 2. Experimental.

**2.1 SAMPLE PREPARATION.** — Dissolution of 117 native Nafion (E. I. du Pont de Nemours, Inc [2]) acidic membrane (EW 1100) has been achieved by using the classical procedure described by Grot [3] and Martin *et al.* [4]: small pieces of membrane are swollen in a 50/50 water-ethanol mixture and heated for 1 h at 250 °C under pressure. The hydroalcoholic homogeneous solution is then carefully concentrated by slow evaporation around 80 °C. Upon evaporation of the solvent, the viscous solution becomes a gel which cracks and forms solid transparent particles when dried. By milling at room temperature in an agate mortar, a fine white powder is obtained that readily dissolves at room temperature in many polar solvents at various concentrations [5]. Samples

(\*) CNRS.

(\*\*) On sabbatical leave from Ritsumeikan University, Chemistry Department, Japan.

with a volume fraction of polymer  $\phi_V$  ranging from 0.28 % to 25 % have been prepared in water, ethanol, N-methylformamide (NMF) and formamide (FA);  $\phi_V$  is deduced from the weight percentage assuming constant bulk densities for all solvents ( $\rho_{\text{water}} = 1$ ,  $\rho_{\text{ethanol}} = 0.785$ ,  $\rho_{\text{NMF}} = 0.999$ ,  $\rho_{\text{FA}} = 1.129$  and  $\rho_{\text{polymer}} \sim 2 \text{ g/cm}^3$ , the density of the starting bulk membrane). The experimental upper limit of the concentration range, which depends upon the solvent, is reached when the sample becomes a stiff gel and bubbles appear when the container is tightly closed.

Lithium samples have also been prepared by exchanging against  $\text{Li}^+$  for 1 h. The native acidic membrane is placed in an aqueous hot solution ( $\sim 90^\circ\text{C}$ ) of  $\text{LiCl}$  1 M; then the same preparative procedure is performed. Lithium and acidic dialyzed samples have been prepared in the same solvents in order to prevent the drying of the colloidal hydroalcoholic starting solution which may possibly induce structural transformations. After dialysis, the solution concentrations are determined by weighing the dry polymer after evaporation by heating between  $80^\circ\text{C}$  and  $150^\circ\text{C}$  depending upon the solvent. Adjustments by dilution are made before the scattering experiments. No difference in the small angle scattering patterns were observed between identical concentrated solutions obtained by these two routes. Most of the solutions studied in this paper were therefore obtained from powders.

**2.2 SMALL ANGLE NEUTRON (SANS) AND X-RAY (SAXS) SCATTERING SPECTROMETERS.** — Samples were examined with the SANS spectrometer PACE (Orphée Reactor of the Leon Brillouin Laboratory, Saclay, France) over a wide range of momentum transfer  $Q$  ( $Q = 4 \pi \sin \theta / \lambda$ ,  $5 \times 10^{-3} \leq Q \leq 2 \times 10^{-1} \text{ \AA}^{-1}$ ) by using the wavelengths  $\lambda$  associated with four sample detector distances  $d$  ( $\lambda = 7 \text{ \AA}$  with  $d = 2.5 \text{ m}$  and  $\lambda = 6.4 \text{ \AA}$  with  $d = 1.4 \text{ m}$  for the high  $Q$  range,  $\lambda = 12 \text{ \AA}$  with  $d = 3.50 \text{ m}$  and  $4.75 \text{ m}$  for the small  $Q$  range). Sample containers were quartz disks separated with 1 mm thick spacers, hermetically closed when fixed in the metallic holder.

SAXS experiments have been performed with the D22 synchrotron radiation spectrometer (DCI, LURE, Orsay, France) over a nearly identical  $Q$  range ( $8 \times 10^{-3} \leq Q \leq 2.8 \times 10^{-1} \text{ \AA}^{-1}$ ) with  $\lambda = 1.549 \text{ \AA}$ . Sample containers consisted of PTFE rings, 1 to 5 mm thick, surrounded by two capton thin films which were held in place by metallic holder.

### 3. Analysis of the results.

**3.1 THE IONOMER PEAK.** — The analysis presented here is consistent with the previous paper [1]. We start from the position  $Q_{\text{max}}$  of the ionomer peak

which is attributed to an interference between the scattering objects and therefore gives a spacing  $d = 2 \pi / Q_{\text{max}}$ . An example of the scattering curve dependence is given in figure 1. The volume fraction of the polymer is obtained from the assumption that the density of the scattering objects is the same as

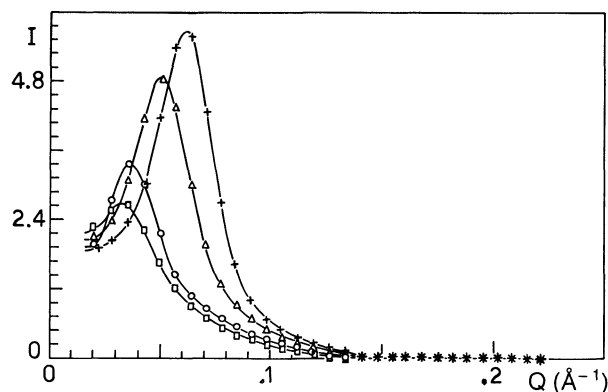


Fig. 1. — Example of the small angle neutron scattering curves obtained for different volume fractions of acidic perfluorinated ionomer in formamide:  $\square$  4.0 %;  $\circ$  5.9 %;  $\triangle$  12.4 %; + 19.5 %; \* For  $Q > 0.14$ , the intensity is zero in every solution.

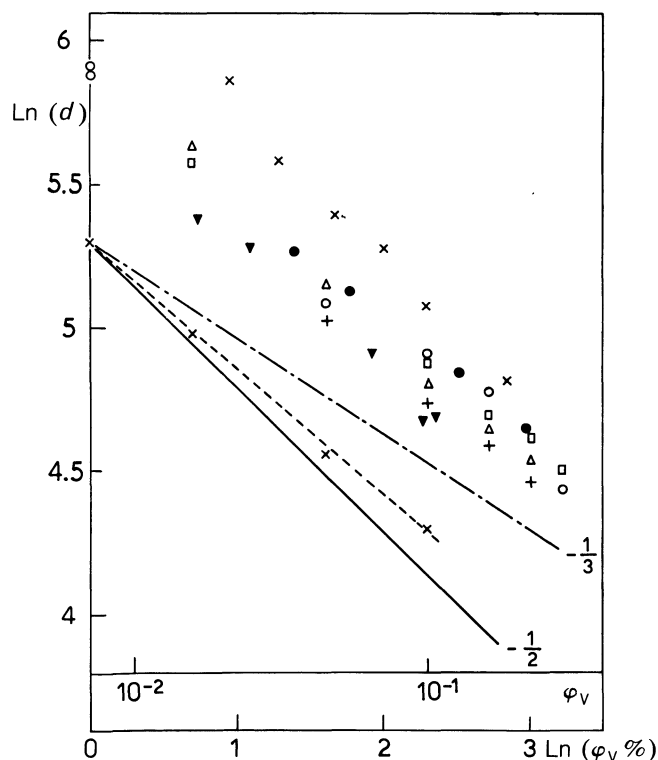


Fig. 2. —  $\text{Ln}(d)$  versus  $\text{Ln}(\phi_V)$  for different solvents. The  $d$  values are obtained from the peak position using the Bragg relation:  $d = 2 \pi / Q_{\text{max}}$ .  $\times$  <sup>(a)</sup>  $\text{H}_2\text{O}$  1 100  $\text{H}^+$ ;  $\Delta$  NMF 1 200  $\text{Li}^+$ ;  $\bullet$  FA 1 100  $\text{H}^+$ ;  $\square$  NMF 1 200  $\text{H}^+$ ;  $\blacktriangledown$  <sup>(a)</sup>  $\text{C}_2\text{H}_5\text{OH}$  1 100  $\text{H}^+$ ;  $\circ$  NMF 1 100  $\text{H}^+$ ; + NMF 1 100  $\text{Li}^+$ ; theoretical slopes and calculated slope (----) from appendix A are indicated. <sup>(a)</sup> These data are taken from previous paper [1].

that of the starting bulk membrane i.e. 2 g/cm<sup>3</sup>. The *d* spacings as a function of φ<sub>v</sub> for different solvents and polymer counterions are given in Table I. In figure 2 is plotted Ln (*d*) versus Ln (φ<sub>v</sub>) for the different samples. If the scattering objects have a constant mass or shape independent of the dilution, one can have an indication on the dimensionality of the arrangement from the slope  $x = -\text{Ln}(d)/\text{Ln}(\varphi_v)$ . A three-dimensional arrangement of isotropic scatterers, like spheres, would give a slope with  $x = 1/3$ ; a two-dimensional arrangement of cylinders or rods would give  $x = 1/2$  and finally  $x = 1$  would correspond to a lamellar structure of sheets. As shown in this figure, the slopes are nearly the same for all series and the averaged value is 0.42, an intermediate value between 0.33 and 0.5.

At this point, it should be noted that the observed intensity is the product of a structure factor  $|F(Q)|^2$ , characteristic of the scattering object and corresponding to a decreasing function of *Q* in the observed *Q* range, by an interference function *S(Q)*. The true values associated with the *S(Q)* maxima are therefore shifted towards lower values of *Q*. A calculation presented in the appendix A shows that this effect has the consequence of lowering the absolute value of the theoretical slope. In the case of a two-dimensional hexagonal lattice with a hard core repulsion, for low concentrations, the overall slope is  $x = 0.43$ . We therefore conclude in favor of a two-dimensional arrangement of rods which must have a perfluorinated hydrophobic core with their surface covered by the SO<sub>3</sub><sup>-</sup> hydrophilic groups.

To obtain microscopic information on the diameter of the rods, one has to assume their density and one has to choose a geometrical arrangement giving a relation between the *d* values and the volume fraction of the polymer. The simplest two-dimensional geometrical arrangements of rods are hexagonal or cubic as already discussed [1]. With the assumption that the density of the rod is about that of the starting bulk polymer, one can therefore define the diameter of the rods and the specific surface [ $\sigma$ ] occupied by one charge on the surface of these rods. We recall some geometrical formulae : in the two-dimensional hexagonal array of rods, the true distance *D* between the nearest neighbor parallel rods is obtained from the equation  $D = 2 \times 3^{-1/2} \times d = 1.155 d$  with  $d = 2 \pi / Q_{\text{max}}$ . From the assumption of cylindrical rods having a density close to 2 g/cm<sup>3</sup>, one gets the radius *r* of the cylinder,  $r = (2 \times 3^{-1/2} \times \pi^{-1})^{1/2} d \varphi^{1/2} = 0.606 d \varphi^{1/2}$ , where  $\varphi = 0.01 \varphi_v$ .

The specific surface  $\sigma$  occupied by one charge on the surface of the rod is given by  $\sigma = 2 V r^{-1}$  where *V* is the polymer volume per unit charge. It is also possible to define the rod length associated with one

Table I. — Table gathering the scattering data obtained for different samples. The *d* values obtained from the peak position and the specific surface associated with one charge are given for different polymer concentrations.

	φ <sub>v</sub> (%)	<i>d</i> (Å)	σ (Å <sup>2</sup> )
1 100 H <sup>+</sup> EtOH (a)	0.4	350	136
	2.1	217	95.8
	3	194	89.5
	6.8	135	85.6
	9.7	108	89.5
	10.5	109	85.3
1 100 H <sup>+</sup> NMF	1	370	81.5
	2	262	81.4
	5	161	84.1
	10	134	71.3
	15	119	65.6
	20	87.3	77.2
	25	84.9	70.9
1 100 H <sup>+</sup> Formamide	4.0	193	78.3
	5.9	168	73.7
	12.4	127	67.5
	19.5	105	65.2
1 100 H <sup>+</sup> H <sub>2</sub> O (a)	3.6	266	59.7
	5.3	219	59.7
	7.5	194	56.7
	9.9	159	60.2
	16.9	123	59.6
	1 100 Li <sup>+</sup> NMF	5	152
10		115	83.1
15		98.7	78.8
20		87.4	77.1
1 200 H <sup>+</sup> NMF	1	359	91.5
	2	262	88.7
	5	170	86.5
	10	131	79.4
	15	110	77.0
	20	103	71.3
	25	89.8	73.2
1 200 Li <sup>+</sup> NMF	2	280	82.9
	5	170	86.7
	10	123	84.8
	15	105	81.2
	20	93.5	78.6

(a) The values of φ<sub>v</sub> and *d* are taken from previous paper [1].

charge  $l = (\pi r^2)^{-1} V$ . In table I a value of  $\sigma$  is given for each sample by considering only the samples for which the concentrations are larger than 0.03 since the location of the peaks becomes uncertain for more diluted solutions. The average value of  $\sigma$  and *r* for each series is summarized in table II. The

Table II. — Table giving the average specific surface  $\bar{\sigma}$ , the radii obtained from geometrical considerations ( $r$ ) and direct measurements ( $R$ ), for different solutions.

	$\bar{\sigma}$ ( $\text{\AA}^2$ )	$r$ ( $\text{\AA}$ )	$R$ ( $\text{\AA}$ )
1 100 H <sup>+</sup> EtOH	87.5	21	18
1 100 H <sup>+</sup> NMF	73.8	25	26
1 100 H <sup>+</sup> FA	71.2	26	27
1 100 H <sup>+</sup> H <sub>2</sub> O	59.2	31	25
1 100 Li <sup>+</sup> NMF	81.9	22	
1 200 H <sup>+</sup> NMF	77.5	26	
1 200 Li <sup>+</sup> NMF	82.8	24	

analysis for a cubic phase of rods would give  $\sigma'$  and  $r'$ ; these values are related to the corresponding values for the two-dimensional hexagonal array of rods by  $\sigma' = 1.861 \sigma$  and  $r' = 0.537 r$ .

**3.2 THE STRUCTURE FACTOR.** — For  $Q > Q_{\max}$ , the interference term should tend towards unity so that  $I(Q)$  in that region should become proportional to  $|F(Q)|^2$ , the structure factor of an isolated scattering object. Direct information on the geometry of these objects can therefore be obtained from the scattering curves of diluted solutions where the peak maximum is shifted towards  $Q$  values smaller than the considered  $Q$  range. If there were small isotropic objects, we should have  $|F(Q)|^2 \cong \exp(-Q^2 R_g^2/3)$  in that  $Q$  region [6, 7], if  $Q \leq 1/R_g$  where  $R_g$  is the radius of gyration ( $R_g^2 = \frac{3R^2}{5}$ ) for an homogeneous sphere of radius  $R$ . If the objects are long cylinders or flat discs whose overall dimension is larger than  $2\pi/Q_{\min} \approx 10^3 \text{\AA}$ , ( $Q_{\min}$  being the minimum experimental  $Q$  value) then in the experimental  $Q$  range the scattered intensity is proportional to  $|F(Q)|^2 = Q^{-n} \exp(-Q^2 R_g^2/(3-n))$  with  $n$  respectively equal 1 or 2.

By drawing plots of  $\text{Ln}[Q^n I(Q)]$  versus  $Q^2$  we have obtained a linear dependence for  $n = 1$  only, which corresponds to the form factor of a long cylinder. A typical example of such plot is shown in figure 3. Such a result is an important confirmation of the above geometrical analysis; it also allows a direct determination of  $R_g$  or of  $R$ , the radius of a homogeneous cylinder:  $R^2 = 2R_g^2$ . The values of  $R$  so obtained are listed in table II together with  $\bar{\sigma}$  and  $r$ .

This absolute determination of  $R$  is very helpful because it allows us to select, among the different two-dimensional arrangements giving values of  $r$  differing only by a proportionality coefficient, the one which gives the best agreement between  $r$  and  $R$  i.e. the hexagonal arrangement. The possibility of a cubic phase of rods has to be excluded since

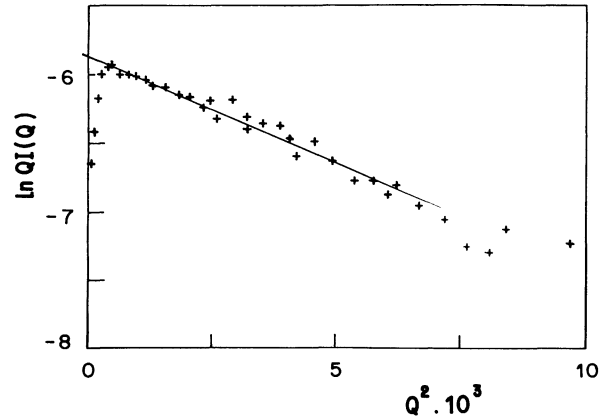


Fig. 3. — Extended Guinier plot of a diluted sample (0.28 % Nafion 1 100 H<sup>+</sup>/FA) showing the rod like structure and giving the radius of the rods from the slope.

$r' = 0.537 r$  gives values too small to fit with the  $R$  values. This conclusion is opposite to the conclusion obtained in our preceding paper [1] from geometrical considerations only and with the hypothesis that each rod contained only one macromolecule; such a hypothesis is probably not realistic and the rods must be made from several polymer chains.

A last remark can be made about the specific surface associated with a charge on the surface of the rod. The value obtained for water solutions is  $59 \text{\AA}^2$ . A very similar value had been obtained in the water swollen starting membrane [8]. The structures of the solutions correspond to micelles compared to the structure of the starting material which form inverted micelles [9, 10] as in many other ionomer systems [11, 12].

#### 4. Discussion.

The results of the analysis led to the conclusion that the solutions consist of long cylinders having a more or less perfluorinated organized core and internal structure with the ionic charges on the surface. Reasonably constant values of the specific surface are obtained when changing the concentration. However the confidence in such a result has to be attenuated because of the experimental uncertainties in the peak position which was taken without any correction. The specific choice of a hexagonal arrangement led to an absolute determination of the geometrical parameter in agreement with the values obtained from the extended Guinier plots of the scattered intensity for the diluted solutions. Anyway the comparison between the values of the specific area obtained in different solvents is independent of the absolute determination. Having obtained a diameter for the rods, the question arises concerning their length. The linear dependence of  $\text{Ln}[QI(Q)]$  versus  $Q^2$  in diluted solutions is valid down to very

small  $Q$  values which gives an inferior limit of  $\sim 10^3 \text{ \AA}$  for the length of the rods. The present status of the experiments does not allow us to give better precision about the length as well as about the diameter distribution.

The choice of the solvents was suggested by their wide range of dielectric constant :  $\epsilon(\text{NMF}) = 180$  ;  $\epsilon(\text{FA}) = 111$  ;  $\epsilon(\text{H}_2\text{O}) = 80$  ;  $\epsilon(\text{C}_2\text{H}_5\text{OH}) = 25$ . The most striking feature is first the relative change of  $\sigma$  from one solvent to another and above all its apparent erratic variation upon  $\epsilon$ . This behaviour is quite different from that observed in polyelectrolytes. In our previous paper [1] we had underlined the importance of the interfacial energy  $\gamma$  between the solvent and the polymer. We have two different series of  $\gamma$  values. The first series corresponds to the interfacial energy between the solvent and air :  $\gamma(\text{C}_2\text{H}_5\text{OH}) = 22 \text{ cgs}$  ;  $\gamma(\text{NMF}) = 39 \text{ cgs}$  ;  $\gamma(\text{FA}) = 58 \text{ cgs}$  ;  $\gamma(\text{H}_2\text{O}) = 72 \text{ cgs}$ . The second series corresponds to the interfacial energy between the solvent and the polytetrafluoroethylene polymer and has been defined from contact angle measurements [16] :  $\gamma(\text{C}_2\text{H}_5\text{OH}) = 3.6 \text{ cgs}$  ;  $\gamma(\text{NMF}) = 19 \text{ cgs}$  ;  $\gamma(\text{FA}) = 21.6 \text{ cgs}$  ;  $\gamma(\text{H}_2\text{O}) = 49.7 \text{ cgs}$ . Figure 4 shows that a linear variation is observed in both cases when plotting  $\text{Ln}(\bar{\sigma})$  versus  $\text{Ln}(\gamma)$  but different slopes are obtained ;  $-1/3$  if one considers the values of  $\gamma(\text{solvent-air})$ ,  $-1/4$  if one considers the values of  $\gamma(\text{solvent-PTFE})$  and if one discards ethanol solutions.

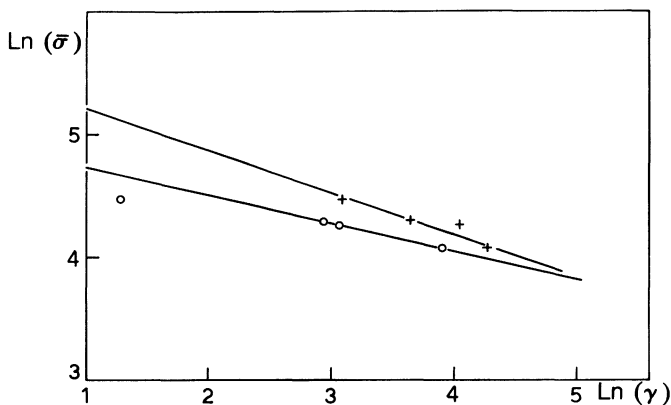


Fig. 4. — Plot of the specific surface associated with one charge versus the interfacial energy between the solvent and respectively the PTFE polymer (O) and the air (+).

The important result is that the radius of the rods, or the specific surface  $\sigma$ , depends on the interfacial energy and not on the dielectric constant. If the surface energy was acting alone, one should observe a collapse of  $\sigma$  or an increase of  $r = 2V/\sigma$ . The problem now is to find the balancing force which prevents such a collapse. One could think, first, about the electrostatic repulsion between the

charges. There are two naive ways to calculate its effect ; the first one is to consider the length  $l$  along the rod associated with one charge and to scale (like in polyelectrolytes) the electrostatic repulsion as  $1/l$  ; the second way is to consider the charges as being distant by  $\sqrt{\sigma}$  on the surface of the rod. The total energy per charge is therefore :

$$E = \gamma\sigma + \frac{A}{\epsilon l} = \gamma\sigma + \frac{A}{\epsilon} \frac{4\pi V}{\sigma^2}$$

in the first case and

$$E = \gamma\sigma + \frac{A'}{\epsilon \sqrt{\sigma}}$$

in the second case. In these equations  $\gamma$  is the interfacial energy,  $\epsilon$  the dielectric constant,  $V$  the volume of polymer per charge,  $A$  and  $A'$  constant values. One can minimize the sum and get the specific surface at equilibrium  $\sigma = K(\epsilon\gamma)^{-\frac{n}{3}}$  with  $n = 1$  in the first case and  $n = 2$  in the second one. In both cases this dependence does not fit with the experimental results. In the appendix B we have estimated the electrostatic energy in the more sophisticated cell model. The conclusion is that its magnitude is not large enough compared with the interfacial energy. It must be emphasized that, if this electrostatic energy does not play a major role in the diameter definition of one rod, it remains fundamental to explain the repulsion between the rods which gives this hexagonal arrangement.

Another possible balancing force we can imagine is of entropic origin due to the large constraints associated with the location of the charged groups on the surface of the rods where the electrostatic self energy is lowered by several tens of kilocalories per mole. It is however difficult to force every charged group on to the surface especially if the diameter is large and if the charged groups are associated with chains whose backbone is located in the center of the cylinder. The theory for such constraints does not exist. It is clear that such an effect opposes the collapse of  $\sigma$  and does not depend on the solvent but depends only on the polymer flexibility, equivalent volume, etc. We just present here a very speculative estimation of this effect which is mainly associated with the elongation of the side chains. As an approximation one can use the formula giving the free energy  $F$  of a Gaussian chain having a free end-to-end distance  $\lambda$ , when it is elongated to a distance  $\rho$  :  $F = \frac{3}{2} kT \frac{\rho^2}{\lambda^2}$ . The elongated distance has to be connected with the radius of the cylinder. For a homogeneous cylinder of radius  $r$ , the average distance of any point to the surface of the cylinder is  $\rho^2 = r^2/6$ . Taking into account the relation  $r = 2V/\sigma$ , one has  $F = kT \frac{V^2}{\sigma^2 \lambda^2}$  as the average

energy per charge. By adding the contribution of the interfacial energy  $\gamma\sigma$ , we obtain by minimization of the sum :  $\sigma = (2kTV^2\lambda^{-2})^{1/3}\gamma^{-1/3}$  which gives a dependence in  $\gamma^{-1/3}$  consistent with the results. A numerical application by taking the following values :  $\gamma = 70$  cgs or  $0.1$  kcal mole $^{-1}/\text{\AA}^2$  ;  $kT = 0.6$  kcal mole $^{-1}$  ;  $\sigma = 60$   $\text{\AA}^2$  ;  $V = 1000$   $\text{\AA}^3$  gives a value of  $7.45$   $\text{\AA}$  for this end to end distance, which value is quite consistent with the length of the side chain. The model also predicts a small variation of the specific surface with the specific volume or equivalent weight :  $\sigma \cong V^{2/3}$ , which dependence is consistent with the measurements. The predicted temperature dependence is  $(T/\gamma)^{1/3}$ . One feature that this model cannot explain is the influence of the neutralization which seems, in the case of Li, to increase the specific surface by 10 %.

### 5. Conclusions.

The new experimental results presented in this paper, together with the analysis of the scattered intensity for  $Q$  values above the ionomer peak domain, have confirmed the presence of cylindrical rods within the perfluorinated ionomer solutions and are in favor of a structure close to a hexagonal array of parallel rods. The diameter of these rods is a few tens of Angstroms and their length is larger than  $\sim 10^3$   $\text{\AA}$ . This hexagonal order does not extend over long distances but rather corresponds to a local order which therefore broadens the interference peak. A tentative picture of such structure is given in figure 5. By using polar solvents covering a large range of dielectric constant, we have found no

correlation between the diameters of the rods and the dielectric constant values. The equilibrium value for the diameter of the rods seems to result mainly from a balance between elastic and interfacial energies. The elastic energy corresponds to the energy needed to form the rod like structure with the perfluorinated groups inside the rod and the ionic charges on the surface. The interfacial energy corresponds to the phobicity of the polymer towards the solvent which therefore tends to lower as much as possible the contact surface between the PTFE and the solvent. The net result from these two contributions is an equilibrium for the diameter which depends mainly on the side group length and on the interfacial energy. The structure that is proposed for these solutions is therefore very different from the *inverse micellar structure* which has been proposed in the starting bulk material [8, 9, 10]. This model can be used as a starting model to understand the structural changes which occur upon reconstruction of the membranes by casting followed by annealing [13].

### Acknowledgments.

This work has been possible through the numerous small angle experiments performed either in the « Laboratoire Leon Brillouin » using the Pace neutron diffractometer or in « LURE » Laboratory using the D22 X-ray spectrometer. Thanks are due to Drs. J. P. Cotton, J. Teixeira and C. Williams for their continuous assistance during this program. One of us (G. Gebel) is indebted to ATOCHEM Company for support.

### Appendix A [17].

We examine here the shift between the *apparent maximum*  $q_m = q_0 + \Delta q$  of the product  $|F(q)|^2 S(q)$  and the *true maximum*  $q_0$  of  $S(q)$ . For that purpose we need a model for  $S(q)$  which has a finite width in the vicinity of the maximum. The paracrystal which gives a numerical relation between  $q$  and  $d$  is of no help since a Bragg peak (a delta function) is not displaced by multiplying with a varying function  $|F(q)|^2$ .

The simplest model is that of a liquid of parallel infinite cylinders with a *hard core* repulsion leading to a correlation cylindrical hole of radius  $a$ . A trivial extension of the Debye calculation [6, 14] for spheres gives :

$$S(q) = 1 - \frac{2\pi a^2 J_1(qa)}{s qa} \quad (\text{A.1})$$

where  $J_1(x)$  is the ordinary Bessel Function of order 1, and  $s$  the average section occupied by one cylinder.

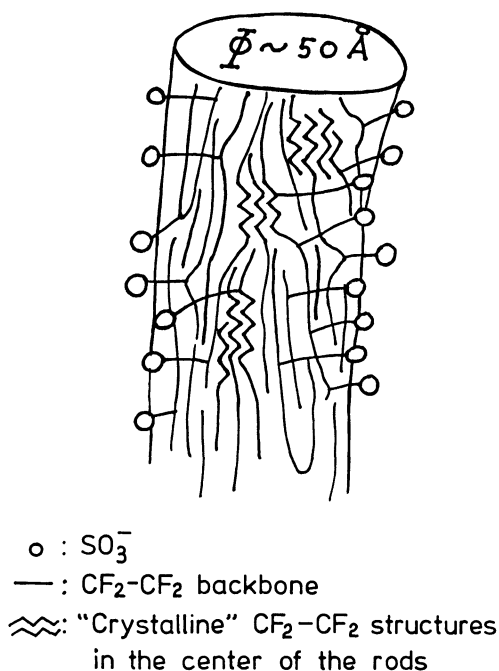


Fig. 5. — Tentative picture of the rod like structure.

The first minimum of  $J_1(x)/x$ , which gives rise to the ionomer peak is located at  $x_0 = 5.2$  where  $J_1(x)/x$  can be approximated by :

$$J_1(x)/x = -0.066 + 3.36 \times 10^{-2}(x - x_0)^2. \quad (\text{A.2})$$

The choice of the numerical coefficient  $2 \pi a^2/s$  will be done in the following way. We first adjust  $a$ , the closest distance, in such a way that the peak coincides with that of a paracrystalline lattice (here we limit ourselves to a hexagonal lattice). As  $q_0 D = 4 \pi 3^{-1/2} = 7.2552$  in the hexagonal lattice (we recall that  $D$  is the distance between rods) and as  $q_0 a = 5.2$  in the hard core model one obtains :

$$a = 0.7167 D. \quad (\text{A.3})$$

This adjustment is quite acceptable, because the electrostatic repulsion  $a$  is not related to  $2 R$  (geometrical contact of the rods), and since  $a = D$  is a too strong statement.

As in the hexagonal lattice  $s = 3^{1/2} D^2/2$  one finds for the ratio  $2 \pi a^2/s$  a numerical value : 3.73 independent of the volumic fraction  $\varphi$  of polymer. One recalls also the relation :

$$\varphi = \pi R^2/s$$

which relates  $\varphi$  to  $D$  or  $a$ , or  $q_0$ .

The structure factor of an infinite homogeneous cylinder [6, 7] of radius  $R$  is given by :

$$|F(q)|^2 \approx q^{-1} \exp\left[-\frac{q^2 R^2}{4}\right]. \quad (\text{A.4})$$

By derivation one solves for  $\Delta q$ , the shift in  $q_m$ . As a first approximation

$$\Delta q = -0.184 q_0 \left(1 + \frac{q_0^2 R^2}{2}\right)$$

or

$$q_m = 0.816 q_0 (1 - 0.113 q_0^2 R^2) \\ = 0.816 q_0 (1 - 1.6360 \varphi)$$

$q_0$  varies like  $\varphi^{1/2}$ .

The logarithm of the term in parenthesis cannot be assigned to a constant slope in function of  $\text{Ln}(\varphi)$ . Nevertheless, for not too large values of  $\varphi$ , for which the first (linearized) approximation may be valid, one can draw a straight line through the calculated points. Between  $\varphi = 10^{-2}$  and  $10^{-1}$ , for example its slope is about  $-0.07$  which gives for  $\text{Ln}(Q_m)/\text{Ln}(\varphi)$  an apparent slope of  $-0.43$ , close to the observed one. The above, rather crude, calculations show simply that the slope for the *apparent maximum*, even for a two-dimensional array of rods, is smaller than 0.5 and lies between 0.5 and 0.33.

### Appendix B.

In this appendix we calculate the effect of dilution on the electrostatic free energy of the system and its possible consequence for the equilibrium radius  $r$  of the rods, or in a more convenient way for the specific area  $\sigma$  of each charge on the interface with the solvent.

The model which is the best adapted to the physical situation described in this paper, is the well known *cell model*, for which we refer to the basic Katchalsky's review [15]. Since it has been often discussed, mainly in its relation with the condensation of the counterion atmosphere, we shall limit ourselves to the numerical calculation of the dilution effect in a solvent of dielectric constant  $\epsilon$ .

The model by itself consists of an infinite cylinder of radius  $r$ .  $V$  is the *equivalent* volume of the polymer or the volume of polymer for one charge,  $l$  the height of the cylinder corresponding to one charge,  $\sigma$  the specific surface,  $\varphi$  the volumic fraction of polymer in the solution. The rod is supposed to be embedded in a cylindrical cell (radius  $R$ ) of solvent containing the mobile counterions. The system is neutral and the electrical field at  $R$  is zero ; this last condition represents in the simplest way the presence of the other rods in the solution.

One has some simple geometrical relations :

$$V = \pi r^2 l ; \quad r = \frac{2V}{\sigma} ; \quad l = \frac{\sigma^2}{4\pi V} \quad (\text{B.1}) \\ \sigma = 2\pi r l ; \quad \varphi = \frac{r^2}{R^2} ; \quad x = \frac{r'}{R}$$

with  $r \leq r' \leq R$ .

The counterions are distributed in a heterogeneous way, being partly attracted by the negatively charged rod. Per height  $l$  (for one charge) we call  $\Gamma(x)$  the probability of finding the cation between  $x$  and  $x + dx$ .  $\pi(x)$  is the fraction of cationic charge between  $x_0 = \varphi^{1/2}$  (the surface of the rod) and  $x$ . One has

$$\pi(x) = \int_{x_0}^x \Gamma(x) dx. \quad (\text{B.2})$$

In terms of  $\Gamma$  and  $\pi$ , the free energy of the system can be calculated as the sum of the electrical density energy, easy to calculate in the cylindrical geometry, and the entropy of the heterogeneous gas of charges. Starting from the entropy of an homogeneous gas of  $n$  particles in a volume  $V$  :

$$S = kn \text{Ln} \left( \frac{V}{n} \right) \quad (\text{B.3})$$

one solves easily for the total free energy of the rod

(per charge) :

$$\frac{G}{kT} = \frac{A}{2} \int_{\varphi^{1/2}}^1 dx \frac{(1 - \pi(x))^2}{x} + \int_{\varphi^{1/2}}^1 dx \Gamma(x) \text{Ln} \left( \frac{\Gamma(x)}{x} \right) - \text{Ln} \varphi - \text{Ln} 2V. \quad (\text{B.4})$$

Here  $A$  is the dimensionless charge parameter  $A = 2e^2/\epsilon l kT$  ( $e$  = electronic charge).

In the calculation of  $G$  one may discard the last term which is constant for a given material.  $G$  is a function of  $\Gamma$ . The minimization of  $G$  leads to

$$A \left( \frac{1 - \pi(x)}{x} \right) + kT \frac{d}{dx} \left( \text{Ln} \frac{\Gamma(x)}{x} \right) = 0 \quad (\text{B.5})$$

which is an unusual form for the Poisson-Boltzmann (P.B.) equation for the counterions. We have developed a numerical procedure to solve this non linear system which is basically the following : one starts with a trial function  $\pi_0$ , from which by using the above equation (B.5) one can get a first approximation  $\Gamma_1$ . This first function is defined up to a multiplication constant  $\lambda_1$  which is fixed so that

$$\pi_1(x) = \int_{\varphi^{1/2}}^x \Gamma_1(x) dx \text{ is normalized or } \pi(1) = 1.$$

Then  $\pi_1$  is used in a second iteration instead of  $\pi_0$ . This procedure avoids the delicate problem of limiting conditions often encountered in the solution of the P.B. equation. At each step  $G$  is calculated. Within a few iterations (most often of the order of ten to twenty) one obtains  $G$  with a precision better than  $10^{-6}$  which allows safely the calculation of its derivatives. The results are shown in figure 6 for values of  $A$  ranging from 0 to 100, and  $\varphi$  from  $0.7$  to  $10^{-3}$ - $10^{-4}$ . It is for  $A = 0$  ( $\epsilon = \infty$ ) that  $G/kT$  varies

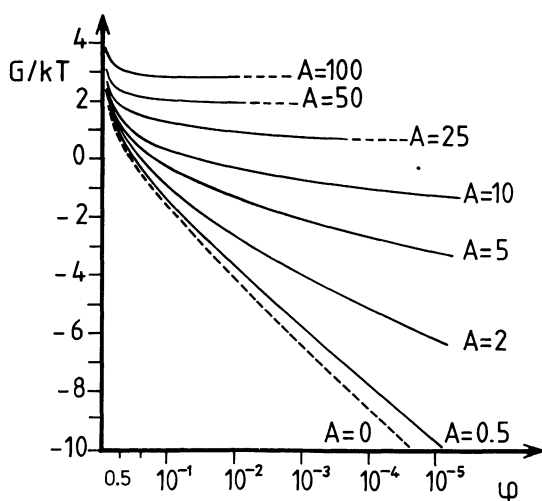


Fig. 6. — Free energy of the rod per charge versus the polymer volume fraction for different  $A$  values ( $A = 2e^2/\epsilon l kT$  where  $e$ ,  $\epsilon$ ,  $k$ ,  $T$  have the usual meanings and  $l$  is the rod height associated with one charge).

the most rapidly with  $\varphi$ . This is expected since in that case the cation gas is free, homogeneous, and expanding. There is no condensation which refrains its expansion.

We need at a given dilution, at constant  $\varphi$ , the variation of  $G$  with  $\sigma$ , or  $l$  or  $A$ . If  $\sigma$  increases, from (B.1),  $l$  increases and  $A$  decreases. One sees on figure 6 that this always leads to a decrease in  $G/kT$ . In other terms the polyelectrolytic effect (electrostatics plus entropy) favors the elongation  $l$  of the rod, or increases  $\sigma$  (in opposition to the interfacial free energy  $\gamma\sigma$ ).

From figure 6 one gets easily the derivative  $d(G/kT)/dA$ , and as

$$\frac{dA}{A} = -\frac{dl}{l} = -2 \frac{d\sigma}{\sigma}$$

it can be easily converted in  $\frac{d}{d\sigma} (G/kT)$ .

We present in figure 7 the results relative to NMF ( $\epsilon = 180$ ). Two series of values are possible depending upon if one chooses the hexagonal arrangement

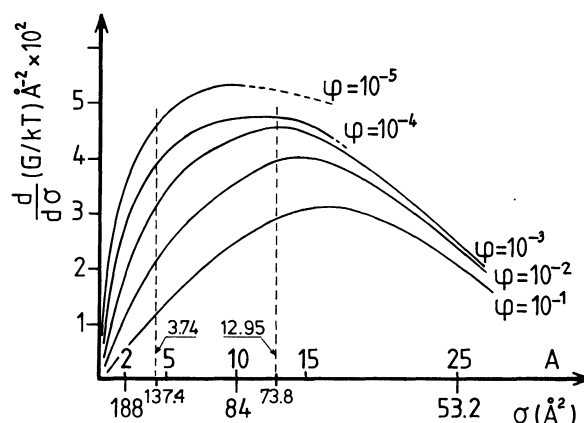


Fig. 7. — Derivative of the free energy versus the specific surface associated with one charge. The curves correspond to the NMF solutions ( $\epsilon = 180$ ) and are plotted for different solution concentrations.

( $A_0 = 12.95$ ) ( $\sigma = 73.8 \text{ \AA}^2$ ) or the cubic phase of rods ( $A_0 = 3.74$ ) ( $\sigma = 137.4 \text{ \AA}^2$ ). For the hexagonal lattice  $\frac{d}{d\sigma} \left( \frac{G}{kT} \right)$  is of the order  $2.4 \times 10^{-2} \text{ \AA}^{-2}$  for  $\varphi = 10^{-1}$  and  $3.4 \times 10^{-2} \text{ \AA}^{-2}$  for  $\varphi = 10^{-2}$ . With  $kT = 0.6$  kcal/mole, the value for the hexagonal lattice corresponds to  $1.44 \times 10^{-2}$  kcal/mole ( $\varphi = 10^{-1}$ ) and  $2.04 \times 10^{-2}$  kcal/mole ( $\varphi = 10^{-2}$ ). Expressed in cgs units, to compare with  $\gamma$ , this gives 10.8 cgs and 14.28 cgs. These values are inferior to the interfacial coefficient with air (39 cgs) or with polytetrafluorethylene (19 cgs).

The situation is the worst for water ( $\epsilon = 80$ ),

$A = 45.44$ ,  $\sigma = 59.1 \text{ \AA}^2$  and for  $\varphi = 10^{-1}$  or  $10^{-2}$  6.72 cgs and 9.45 cgs are found respectively.

For ethanol ( $\epsilon = 25$ ),  $A = 66.3$ ,  $\sigma = 87.5 \text{ \AA}^2$ , the large value of  $A$  leads to a strong condensation of the counterions close to the rod and a poor convergency of our numerical iterations at small dilution. We estimate a very small effect, at most of the order of 1 cgs.

In conclusion of this appendix we see that the polyelectrolytic effect is not in  $1/\epsilon$  as a naive argument would predict. It is in fact stronger for large  $\epsilon$  and this is linked to a weaker condensation of the counterions. We have not found in any case that the polyelectrolytic effect could oppose the surface effect ; at most, it can reduce by a small amount the bare value of  $\gamma$ .

#### References

- [1] ALDEBERT, P., DREYFUS, B. and PINERI, M., *Macromolecules* **19** (1986) 2651.
- [2] E. I. du Pont de Nemours, Inc. Nafion Perfluorinated Membranes (product literature), Feb. 1, 1984.
- [3] GROT, W. G. and CHADDS, F., European Patent 0066369, 1982.
- [4] MARTIN, C. R., RHOADES, T. A. and FERGUSON, J. A., *Anal. Chem.* **54** (1982) 1639.
- [5] ALDEBERT, P. and PINERI, M., French Patent 8605792 (1986).
- [6] GUINIER, A., FOURNET, G., Small angle scattering of X-rays. John Wiley Ed., New York (1955).
- [7] (a) GLATTER, O. and KRATKY, O. in Small-Angle X-Ray Scattering (Academic Press, New York) 1982.  
(b) VAINSHEIN, B. K. in Diffraction of X-rays by chain molecules (Elsevier, New York) 1966.
- [8] DREYFUS, B. in Structure and Properties of ionomers, NATO ASI Series Pineri, M. and Eisenberg, A. Ed., **198** (1987) 27-37.
- [9] GIERKE, T. D., MUNN, G. E., WILSON, F. C., *J. Polym. Sci. Polym. Physics* **19** (1981) 1687.
- [10] ROCHE, E. J., PINERI, M., DUPLESSIX, R., *J. Polym. Sci. Polym. Physics* **20** (1982) 481.
- [11] EISENBERG, A., KING, M., Ion-containing polymers : Academic Press, New York (1977).
- [12] MCKNIGHT, W. J., TAGGART, W. P., STEIN, R. S., *J. Polym. Sci. Symp.* n° 45 (1974) 113.
- [13] GEBEL, G., ALDEBERT, P., PINERI, M., *Macromolecules* **20** (1987) 1425.
- [14] DEBYE, P., *Phys. Z.* **28** (1927) 135.
- [15] KATCHALSKY, A., *Pure and applied Chemistry* **26** (1971) 327.
- [16] ESCOUBES, M., Private communication.
- [17] For convenience in the appendix we use the notation  $q$  instead of  $a$  and  $\varphi$  instead of  $\varphi_v$ .